

Copper Nanoparticle-Doped Silica Cuprous Sulfate as a Highly Efficient and Reusable Heterogeneous Catalysis for N-Arylation of Nucleobases and N-Heterocyclic Compounds

Mohammad Navid Soltani Rad,^{*a} Somayeh Behrouz,^{*a} Mohammad Mahdi Doroodmand,^{b,c} Noushin Moghtaderi^a

^a Department of Chemistry, Shiraz University of Technology, Shiraz 71555-313, Iran

Fax +98(711)7354520; E-mail: soltani@sutech.ac.ir; E-mail: behrouz@sutech.ac.ir

^b Department of Chemistry, College of Sciences, Shiraz University, Shiraz 71454, Iran

^c Nanotechnology Research Institute, Shiraz University, Shiraz, Iran

Received 28 July 2011; revised 17 August 2011

This paper is dedicated to Professor Gholam Hossein Hakimelahi who devotes himself to the progress of medicinal chemistry in Iran.

Abstract: A facile and simple protocol for Ullmann-type N-arylation of nucleobases with aryl halides is described using copper nanoparticle-doped silica cuprous sulfate (CN-DSCS) as a new and efficient heterogeneous catalysis. In this method, treatment of various nucleobases and aryl halides in the presence of DBU and CN-DSCS in refluxing DMF furnishes the corresponding *N*-aryl adducts in reasonable to good yields. The CN-DSCS was fully characterized by different microscopic, spectroscopic and physical techniques, including scanning electron microscopy (SEM), transmission electron microscopy (TEM), atomic force microscopy (AFM), X-ray diffraction (XRD), inductively coupled plasma (ICP) analysis, thermogravimetric analysis (TGA), and FT-IR. The CN-DSCS was proved to be a chemically and thermally stable, cheap, and environmentally compatible heterogeneous nanocatalyst that can be reused for many consecutive experiments without any considerable decrease in its reactivity.

Key words: CN-DSCS, heterogeneous catalysis, Ullmann-type reaction, N-arylation, nucleobase

The high cost, toxic effects, and the problem of waste disposal associated with many transition metals have led to an increased attention toward the development of heterogeneous catalysts. The immobilization of active catalysts on the heterogenous supports provides certain additional characteristics, including selectivity, thermal stability, ease of separation from the reaction mixture, recyclability, and reusability of catalysts.^{1–4} Being one of the most versatile metals for catalysis, copper has been widely employed in a variety of organic reactions. The copper(I)-catalyzed Huisgen's 1,3-dipolar cycloaddition reaction⁵ and Ullmann-type coupling of various nucleophiles with aryl halides are the most distinguished organic transformations using copper catalysts.⁶

Polymers,⁷ charcoal,⁸ cellulose,⁹ zeolites,¹⁰ alumina,¹¹ and silica gel¹² have been widely used as the solid supports in the preparation of copper catalysts. Among the applied solid supports for the preparation of heterogeneous catalysts, silica gel is usually preferred. Silica gel exhibits many advantageous properties, including high surface

area, excellent stability (chemical and thermal), good accessibility, and the environmental compatibility. Additionally, the organic functionalities can be robustly anchored to the surface of silica gel to provide the appropriate catalytic centers.^{13,14} The modified silica gels having NH₂, SH, diamines, and amino acids groups have shown to be the suitable supports for bonding with various transition metals like Pd, Cu, Sc, Ru, Pt, V, etc. useful in many organic synthesis.¹⁵

The ability to construct N-arylated N-heterocycles is currently an active area in organic synthesis due to their prevalence in many natural products and pharmaceutically promising compounds.¹⁶ Among them, *N*-aryl nucleobases have been paid the considerable attention as therapeutics, molecular tools, and probes for investigating the biological systems.¹⁷ The synthesis of *N*-aryl nucleobases generally involves, (i) the heterocyclization of suitable precursors,¹⁸ (ii) the reaction of nucleobases with diaryliodonium salts,¹⁹ and (iii) nucleophilic aromatic substitution (S_NAr) reactions of electron-deficient aryl halides with nucleobases.²⁰ Recently, arylboronic acids in the presence of simple cupric salts have been frequently used for the direct N-arylation of nucleobases.²¹ However, drawbacks such as low yields of product, long reaction time, the use of expensive or less available arylboronic acids, low selectivity, oxidation, and deboronation of arylboronic in the presence of copper(II) and H₂O are usually observed in the above methods. On the other hand, when free copper cation is applied, the complexation of purine nucleobase (i.e., adenine) with copper salt is likely. Hence, there is still an urgent demand for establishing a novel and efficient method for easy accessing the *N*-aryl nucleobases. In the light of wide diversity and availability of aryl halides compared with arylboronic acids, the direct N-arylation of nucleobases with the aryl halides seems to be a suitable and attractive strategy.

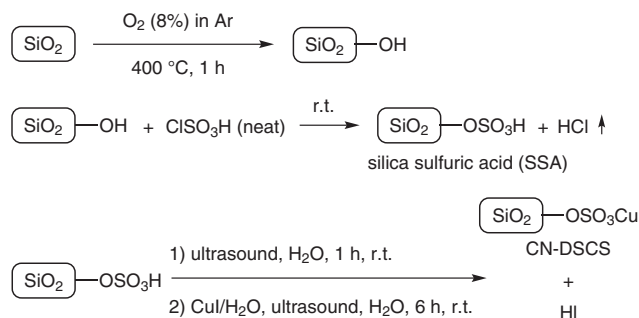
In continuation of our ongoing research on nucleoside chemistry,²² we disclose here the design and synthesis of copper nanoparticle-doped silica cuprous sulfate (CN-DSCS) (Scheme 1) as a novel and efficient heterogeneous catalyst for the Ullmann-type N-arylation of nucleobases and/orazole derivatives with aryl halides (Scheme 2).

SYNTHESIS 2011, No. 23, pp 3915–3924

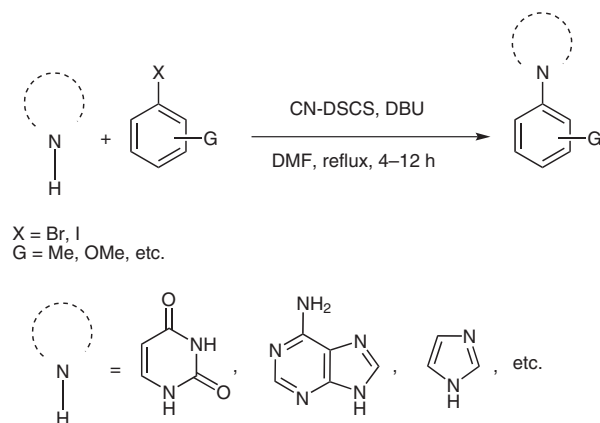
Advanced online publication: 21.09.2011

DOI: 10.1055/s-0030-1260236; Art ID: Z74311SS

© Georg Thieme Verlag Stuttgart · New York



Scheme 1 Routes to prepare the copper nanoparticle-doped silica cuprous sulfate (CN-DSCS)



Scheme 2 Ullmann-type N-arylation of nucleobases and/or azole derivatives with aryl halides using CN-DSCS

Preparation of CN-DSCS

The process for the preparation of CN-DSCS is shown in Scheme 1. According to Scheme 1, the synthesis of CN-DSCS is carried out from freshly prepared silica sulfuric acid (SSA). The preparation of SSA was previously reported by mixing the normal SiO₂ and ClSO₃H.^{23a} However, to our experience, more pleasant result was obtained when activated SiO₂ was used to react with ClSO₃H. In this context, the silica was first activated by a flow of 8% O₂ in argon atmosphere for 1 hour at 400 °C in a furnace. Then, the activated SiO₂ was introduced to an adequate amount of ClSO₃H. Slightly excess of ClSO₃H was added to ensure the enrichment of all active site (i.e., OH) on SiO₂. At this stage, no further HCl gas was evolved. The amount of H⁺ in SSA was determined by simple acid–base back-titration. The amount of H⁺ in SSA was evaluated to be 0.05 gram (0.13 mmol) of silica sulfuric acid.^{23b}

On this basis, CN-DSCS was synthesized from a suspension of SSA in demineralized water, which was primarily exposed to ultrasonic irradiation at room temperature for one hour. A solution of copper(I) iodide in demineralized water, which was previously enriched with portions of NaI solution (see the experimental section) was then mixed with SSA and the mixture exposed to ultrasonic irradiation for six hours at ambient temperature. Filtration followed by washing and drying provided CN-DSCS as a dark-powdered solid (Figure 1).



Figure 1 (a) SiO₂, (b) SSA and (c) CN-DSCS

Characterization of Catalysis Nanostructure

Figures 2, 3, and 4 indicate the scanning electron microscopy (SEM), transmission electron microscopy (TEM), and atomic force microscopy (AFM) images of CN-DSCS, respectively. Good correlation was observed for copper nanoparticles characterized by different microscopic techniques. In addition, the histogram diagram (Figure 5) presents the frequent distribution of CN-DSCS based on the AFM image (Figure 4). Regarding this histogram, the maximum diameter distributed for the copper catalyst is around 25 nm. The X-ray diffraction (XRD) pattern of CN-DSCS is shown in Figure 6. Based on the XRD pattern, the strong peaks corresponds to copper nanostructure, for which the related data are summarized in Table 1.

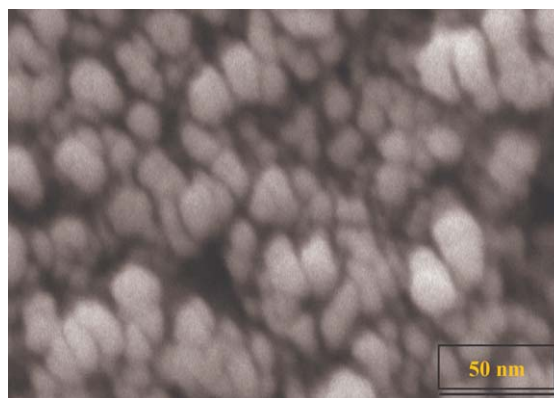


Figure 2 Scanning electron microscopy (SEM) image of CN-DSCS

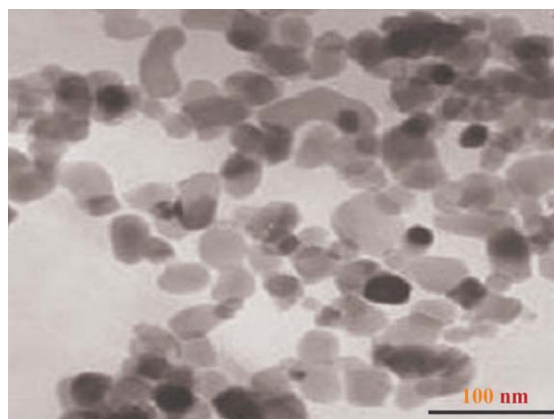


Figure 3 Transmission electron microscopy (TEM) image of CN-DSCS

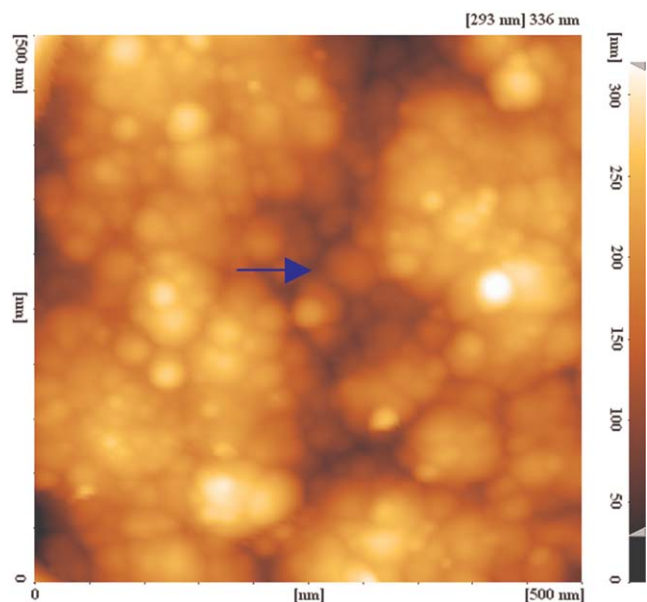


Figure 4 Atomic force microscopy (AFM) image of CN-DSCS

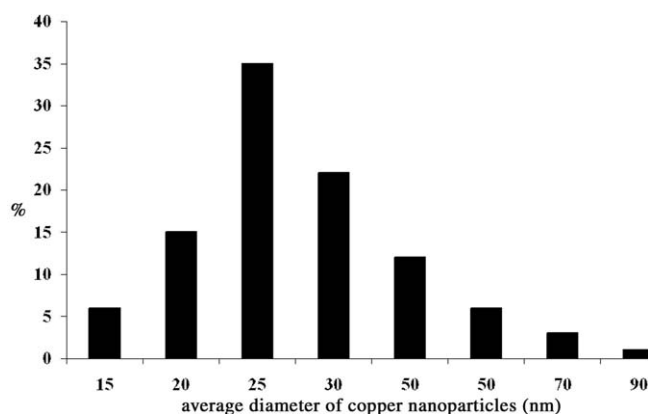


Figure 5 Histogram diagram representing the average diameter of CN-DSCS

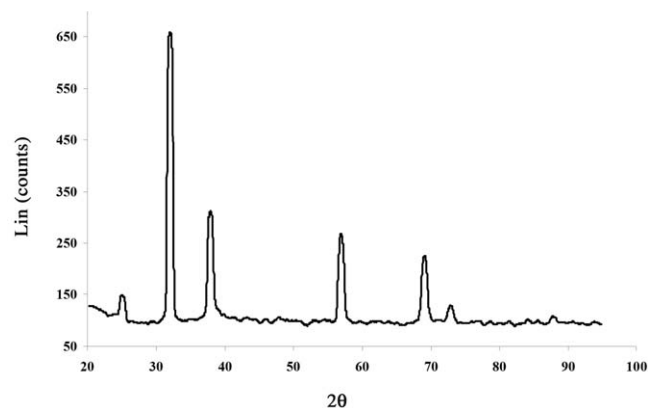


Figure 6 Smoothed X-ray diffraction (XRD) pattern of CN-DSCS

From Table 1, the peak corresponds to the plane of (111) indicates the copper(0) formation in relation with the disproportionation reaction of copper(I) in a polar solution.

Table 1 Analysis of XRD Patterns Related to CN-DSCS after Re-using for Three Times

2θ	Matrix and morphology		Ref.
	Cu	Cu(I)	
25.5	–	(111)	8
30.5	–	(200)	8a
38.5	(111)	(220)	8a
57.2	–	(222)	7
68.5	–	(331)	7
72.1	–	(420)	10a

The copper nanoparticle size was also recognized from X-ray line broadening using Debye–Scherrer formula as: $D = 0.9 \lambda / \beta_{1/2} \cos \theta$, where D , λ , $\beta_{1/2}$, and θ are the average crystalline size, the applied X-ray wavelength, the angular line width at half maximum intensity, and the Bragg's angle, respectively.²⁴

With regard to the peak of copper nanoparticles and the corresponding plane of copper (200) for $\lambda = 1.085 \text{ \AA}$, the average size of copper nanoparticles is estimated at around 28 nm, which is in good agreement with the results attained by the microscopic techniques.

Figure 7 indicates the thermogravimetric analysis (TGA) of CN-DSCS. Based on the TG thermogram, a decrease in weight of CN-DSCS is observed at temperature around 95 °C and it is attributed to desorption of water and other species from CN-DSCS. The decrease in weight is also observed around 230 °C related to desorption of sulfur from CN-DSCS and formation of sulfur dioxide. Furthermore, the increase in weight around 380 °C is also rationalized to the oxidation of copper nanoparticles and formation of copper oxides. The sharp decrease in weight at 850 °C is assigned to the decomposition of silica matrix. Finally, the last part of the thermogram (the flexure obtained at the low weight percentages) shows the quantity of copper oxide and reveals the amount of copper nanoparticles on silica. The estimated value was 6.12%.

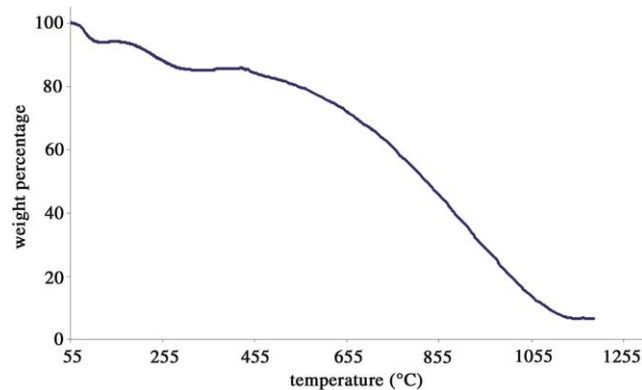


Figure 7 Thermogravimetric (TG) analysis of CN-DSCS

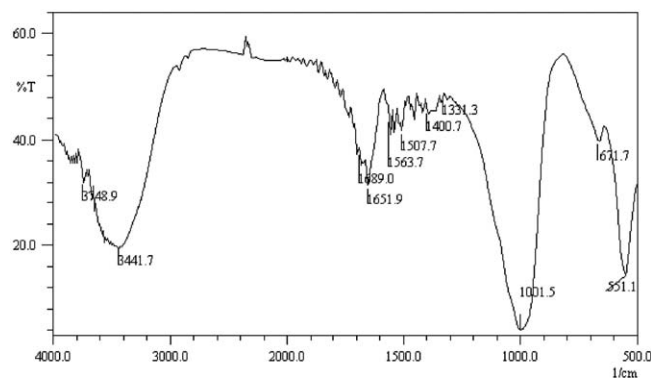


Figure 8 FT-IR spectrum of freshly prepared CN-DSCS

The FT-IR spectrum of the CN-DSCS catalyst is shown in Figure 8. The solid state IR spectrum of catalyst was recorded using the KBr disk technique. Metal oxides generally give absorption bands below 1000 cm^{-1} and in this case, an asymmetric band at 551 cm^{-1} corresponds to Cu–O bond. Furthermore, a band at 671 cm^{-1} is assigned to S–O stretching. A major broad-sharp peak at $900\text{--}1200\text{ cm}^{-1}$ is a set of overlapped bands consisting of several signals, including symmetric and antisymmetric stretching modes of Si–O–Si, asymmetric and symmetric stretching modes of O=S=O, and also symmetric band of Cu(I or II)–O bonds.²⁵

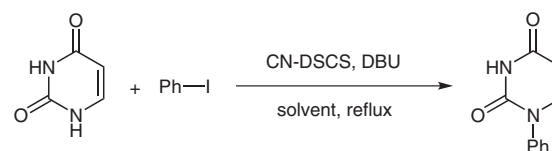
The bands at $1500\text{--}1700\text{ cm}^{-1}$ correspond to water molecules adsorbed on CN-DSCS and combination of the CN-DSCS vibration modes. The spectrum also shows the absorption around 3441 cm^{-1} , which is assigned to stretching vibration of different types of hydroxyl groups.

Ullmann-Type N-Arylation of Nucleobases Using CN-DSCS

After synthesis and characterization of the CN-DSCS, the catalytic activity of CN-DSCS in the Ullmann-type N-arylation reactions of various N-heterocyclic compounds was examined. In this context, many structurally diverse nucleobases and/or azole derivatives were coupled in the presence of 1,8-diazabicyclo[5.4.0]undec-7-ene (DBU) in refluxing DMF (Scheme 2).

The first step of this synthetic approach was started by optimizing the reaction conditions. The coupling of uracil and iodobenzene was chosen as a model reaction. Initially, the effect of various solvents on the model reaction using CN-DSCS (0.3 g, 0.05 mol%), and DBU was studied (Table 2). The results in Table 2 show that the type of solvent has a significant role in the progress of the reaction. Among the examined solvents, DMF (Table 2, entry 4) demonstrated the best result and it was the solvent of choice for all reactions. Use of aprotic solvents, like NMP, DMSO, and HMPA (entries 2, 3, and 5) resulted in moderate yields of *N*-phenyluracil. Other solvents were not suitable enough to progress the reaction, even if the reaction time was allowed to be prolonged.

Table 2 Effect of Various Solvents on the Conversion of Uracil into *N*-Phenyluracil Using CN-DSCS



Entry	Solvent	Time (h)	Yield (%) ^a
1	MeCN	18	10
2	NMP	10	43
3	DMSO	9	51
4	DMF	8	60
5	HMPA	10	45
6	toluene	24	NR ^b
7	THF	24	NR ^b

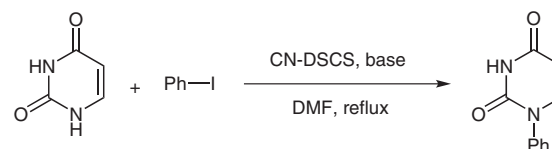
^a Isolated yield.

^b No reaction.

The choice of base for activation of nucleobases is of great significance. We tested the potency of several organic and inorganic bases on the model reaction (Table 3). From the results shown in Table 3, among the examined bases, DBU (Table 3, entry 6) was found to be the best base for the progress of the reaction, whereas K_2CO_3 , Cs_2CO_3 , and DBN (entries 2, 3, and 7) afforded moderate yields of *N*-phenyluracil. Other bases applied in the experiment did not demonstrate any satisfactory results.

The temperature has undeniable role in the improvement of Ullmann type coupling reactions. Therefore, to examine the effect of temperature, the model reaction was con-

Table 3 Effect of Various Bases on the Conversion of Uracil into *N*-Phenyluracil Using CN-DSCS



Entry	Base	Time (h)	Yield (%) ^a
1	MgO	24	trace
2	K_2CO_3	9	55
3	Cs_2CO_3	9	52
4	DABCO	16	10
5	DMAP	16	15
6	DBU	8	60
7	DBN	10	45
8	Et_3N	10	37

^a Isolated yield.

ducted at different temperatures. Increases in temperature remarkably affected the Ullmann-type N-arylation rate and considerably improved the yield of corresponding *N*-phenyluracil. The admissible result was obtained when the coupling reaction was carried out in refluxing DMF for eight hours yielded *N*-phenyluracil in 60%.

The optimized stoichiometric ratios of nucleobase/aryl halide/DBU for the conversion of uracil into *N*-phenyluracil were found to be 1:1.3:2. One should be aware of employing the correct aryl halide ratio. The increment in the mole ratio of aryl halide can lead to the formation of biaryl adducts in the presence of copper(I).

To realize the scope of this protocol, the optimized reaction condition was applied to diverse nucleobases and aryl halides (Table 4). According to Table 4, CN-DSCS proved to be an efficient nanocatalysis for coupling of various aryl halides ($X = \text{I}, \text{Br}$) with purine and pyrimidine nucleobases in reasonable to good yields. All synthesized compounds were fully characterized, and their structures were confirmed by spectroscopic analysis methods, including ^1H and ^{13}C NMR, elemental analysis, mass, IR spectroscopy or compared to those of authentic samples.

Table 4 Ullmann-Type N-Arylation of Nucleobases and/or Azole Derivatives Using ArX/CN-DSCS/DBU in Refluxing DMF

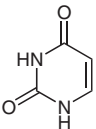
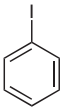
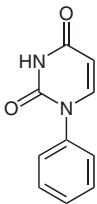
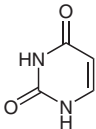
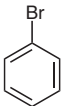
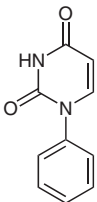
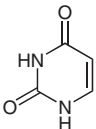
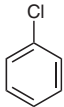
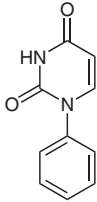
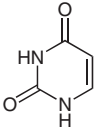
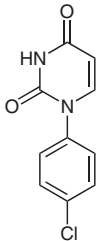
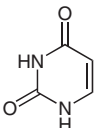
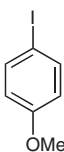
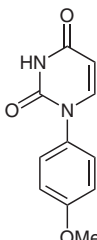
Entry	Nucleobase	ArX	Product ^a	Time (h)	Yield (%) ^b
1 ^{19,21f}				8	60
2 ^{19,21f}				9	56
3 ^{19,21f}				72	trace
4 ^{19b}				8	58
5 ^{19b,21f}				7	61

Table 4 Ullmann-Type N-Arylation of Nucleobases and/or Azole Derivatives Using ArX/CN-DSCS/DBU in Refluxing DMF (continued)

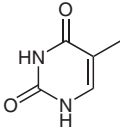
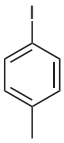
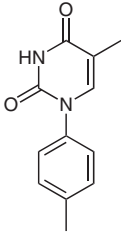
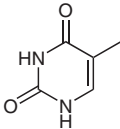
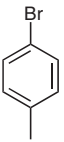
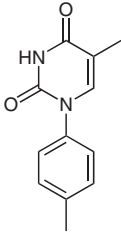
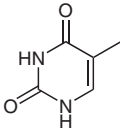
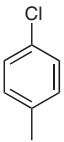
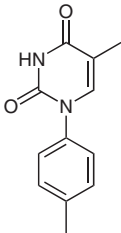
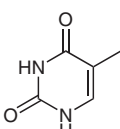
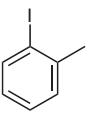
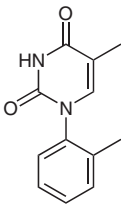
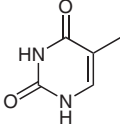
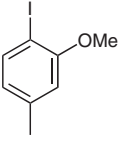
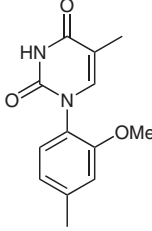
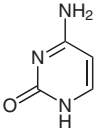
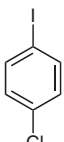
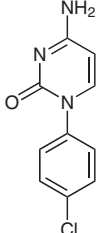
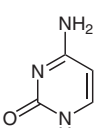
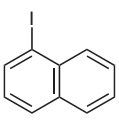
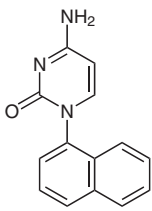
Entry	Nucleobase	ArX	Product ^a	Time (h)	Yield (%) ^b
6 ^{19b,21f}				9	52
7 ^{19b,21f}				11	49
8 ^{19b,21f}				72	trace
9 ^{21f}				12	35
10 ^{21f}				12	38
11 ^{21c}				8	55
12 ^{21c}				8	53

Table 4 Ullmann-Type N-Arylation of Nucleobases and/or Azole Derivatives Using ArX/CN-DSCS/DBU in Refluxing DMF (continued)

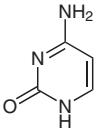
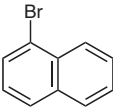
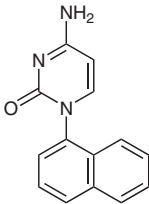
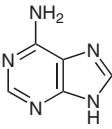
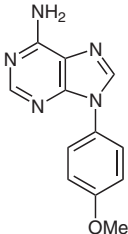
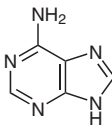
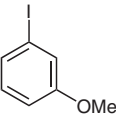
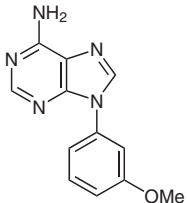
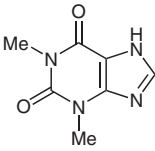
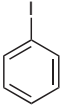
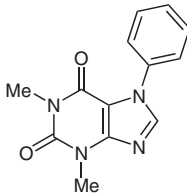
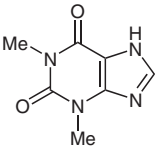
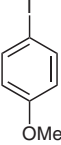
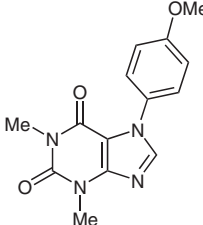
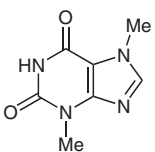
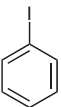
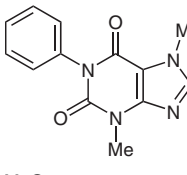
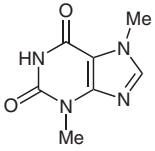
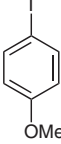
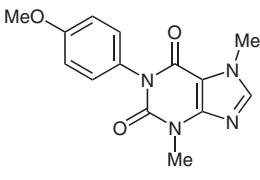
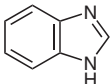
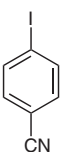
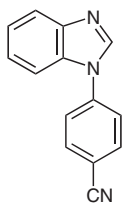
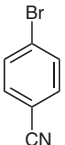
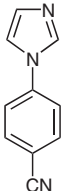
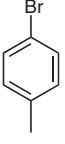
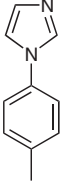
Entry	Nucleobase	ArX	Product ^a	Time (h)	Yield (%) ^b
13 ^{21c}				10	50
14 ^{21c,e,f}				12	48
15 ^{21f}				12	45
16 ^{18g,21i}				6	65
17 ^{26a}				6	67
18				7	67
19				7	68
20 ^{26b}				6	70

Table 4 Ullmann-Type N-Arylation of Nucleobases and/or Azole Derivatives Using ArX/CN-DSCS/DBU in Refluxing DMF (continued)

Entry	Nucleobase	ArX	Product ^a	Time (h)	Yield (%) ^b
21 ^{26b}				4	74
22 ^{26b}				4	77

^a All products were characterized by ¹H and ¹³C NMR, IR, CHN, and MS analysis. For known compounds they were consistent with those reported in the literature (cf. references provided in the entry).

^b Isolated yield.

From Table 4, aryl halides (X = I, Br) having both electron-rich or electron-deficient residues can undergo the Ullmann-type N-arylation of nucleobases. Use of chlorobenzene as an arylating agent led to poor yields of desired products (Table 4, entries 3, 8). The low yields corresponded to aryl chlorides are attributed to higher bond dissociation energy. For example, when both chlorine and iodine are present on aryl ring, only iodine atom is replaced by nucleobase (Table 4, entries 4, 11). The lower yields attained by the *ortho*-substituted aryl iodides compared with other aryl iodides is naturally correlated to steric hindrance present at *ortho* substituents (Table 4, entries 9 and 10). Moreover, there was no considerable discrepancy between the reactivity of aryl iodides and aryl bromides for nucleobases in our experiment. To illustrate the scope of this method, the optimized reaction conditions were also applied to other N-heterocycles including benzimidazole and imidazole.

Good yields of the corresponding adducts were obtained using CN-DSCS (Table 4, entries 20–22). Good regioselectivity was also observed in the N-arylation of nucleobases using CN-DSCS. The N-arylation of purine and pyrimidine nucleobases was chiefly achieved at N9 and N1 sites respectively, whereas the corresponding *N*⁷-aryl for purines and/or *N*¹,*N*³-diaryl derivatives for pyrimidines were obtained in trace amounts (<5%).

Reusability of CN-DSCS

The reusability of the CN-DSCS was studied during the synthesis of *N*-phenyluracil (Table 5, entry 1). In this context, prior to use and also final testing of the catalyst for determination of its activity in many subsequent runs, the catalyst was recycled from the reaction mixture through a sintered glass funnel (vacuum filtration). The catalyst was then washed successively with THF (three times) and dried in a vacuum oven at 100 °C for 30 minutes. The catalyst was tested for five consecutive runs and through each run, no fresh catalyst was added. As the results in

Table 5 indicate, the catalyst can be reused for many consecutive runs without remarkable decrease in its catalytic reactivity.

Table 5 Reusability of CN-DSCS in Successive Trials for the Synthesis of *N*-Phenyluracil

Run	Time (h)	Yield (%) ^a
1	8	60
2	8	58
3	9	53
4	9.5	49
5	10	47

^a Isolated yield.

To prove the recoverability and demonstrate the thermal as well as chemical stability of CN-DSCS, analytical techniques such as inductively coupled plasma (ICP) and TGA instrument were used for measuring the copper amounts before and after five successive uses of CN-DSCS. Based on the ICP results, the amount of copper bonded on fresh CN-DSCS was evaluated to 6.12%. This value was also calculated to 6.14%, according to TG analysis. The small difference between obtained results from ICP and TGA analyses is attributed to sample pretreatment before ICP analysis. Based on the ICP results, the amount of copper species was diminished to 6.11% after five sequential reuses. The ICP analysis has revealed the capability of applied procedure for synthesis of copper nanoparticles. Additionally, the ICP analysis has en-

dorsed the recoverability of CN-DSCS without significant leakage from the silica matrix. As it is well indicated, the amount of leached copper from CN-DSCS is negligible (0.01% after five runs) and it is reasoned due to strong ionic bonds present between copper cations and sulfate group on the surface of SSA. This characteristic of CN-DSCS demonstrates its superiority in comparison with usual catalysts, which normally are prepared by immobilization of copper species on solid supports and/or polymers.

In summary, we have described the preparation and characterization of copper nanoparticle-doped silica cuprous sulfate (CN-DSCS) as a highly efficient heterogeneous catalysis for Ullmann-type N-arylation of nucleobases with aryl halides. In this synthetic methodology, CN-DSCS was proved to be a useful catalyst for coupling of purines, pyrimidines, and/or azoles derivatives with ArX (X = Br, I) in the presence of DBU and DMF. Using CN-DSCS, reasonable to good yields of N-aryl heterocyclic adducts were obtained in favorable regioselectivities. CN-DSCS demonstrates to be an efficient, thermally and chemically stable, environmental compatible, and low cost catalysis that can be easily prepared, recycled, and reused for many consecutive runs without decrease in the catalytic reactivity.

All preliminary chemicals were purchased from Fluka, Merck, and/or Sigma-Aldrich. Preparation of SSA was conducted according to the procedure in literature.²³ Solvents were purified and dried by standard procedures, and stored over 3 Å molecular sieves. Reactions were followed by TLC using SILG/UV 254 silica-gel plates. Column chromatography was performed on silica gel 60 (0.063–0.200 mm, 70–230 mesh, ASTM). The TGA of CN-DSCS was analyzed using a lab-made thermogravimetric (TG) analyzer instrumentation system. The transmission electron microscopy was employed using TEM (CN-10, Philips, 100 KV). The scanning electron micrograph was attained using SEM (XL-30 FEG, Philips, 20 KV) instrument. An atomic force microscopy (AFM, DME-SPM, version 2.0.0.9) was also used for AFM image. Spectroscopic techniques such as inductively coupled plasma (ICP) and patterned X-ray diffraction (XRD, D8 Advance, Bruker AXS) were employed for characterization of CN-DSCS. Melting points were measured using a Büchi-510 apparatus in open capillaries and are uncorrected. FT-IR spectra were obtained using a Shimadzu FT-IR-8300 spectrophotometer. ¹H and ¹³C NMR spectrum was attained using a Bruker Avance-DPX-250 spectrometer operating at 250/62.5 MHz, respectively (δ in ppm, J in Hz). GC/MS were performed on a Shimadzu GC/MS-QP 1000-EX apparatus (m/z, %). Elemental analyses were conducted on a Perkin-Elmer 240-B microanalyzer. Full analytical data are provided for novel products and references are given for known compounds (Table 4).

Copper Nanoparticle-Doped Silica Cuprous Sulfate (CN-DSCS)

For the preparation of CN-DSCS, SSA (3.0 g) was dispersed in triply distilled H₂O (50 mL). The suspension was then sonicated for 1 h in a beaker inside a sonication bath (frequency 100 MHz, 80 W) at r.t. The suspension was left for about 30 min to be deposited and separated. An aqueous solution of 1.0 mM of CuI was prepared by dissolving CuI in triply distilled H₂O (100 mL) and it was enriched by the addition of 0.02 M aq NaI (10 mL). Then, this solution was added to the SSA dropwise, during which the suspension was sonicated in a beaker inside a sonication bath (frequency 100 MHz, 80

W) at r.t. After filtration of CN-DSCS, the dark solid reagent was washed by distilled H₂O (3 × 10 mL). The CN-DSCS was then dried under vacuum at 80 °C.

Ullmann-Type N-Arylation of Nucleobases; General Procedure

In a double-necked 100 mL round-bottomed flask equipped with a condenser was added a mixture consisting of appropriate nucleobase or other N-heterocycle (0.01 mol), DBU (0.02 mol), aryl halide (0.013 mol), and CN-DSCS (0.3 g, 0.05 mol%) in DMF (30 mL). The mixture was heated at reflux, and in most cases, darkening of reaction media had occurred. Heating was continued until TLC indicated no further progress in the conversion (Table 4). Then, the catalyst was filtered off and the filtrate was evaporated under vacuum to remove the solvent. The remaining foam was dissolved in CHCl₃ (100 mL) and subsequently washed with H₂O (2 × 100 mL). The organic layer was dried (Na₂SO₄) and evaporated. The crude product was purified by column chromatography on silica gel eluting with proper solvents (Table 4).

3,7-Dimethyl-1-phenyl-1H-purine-2,6(3H,7H)-dione (Table 4, entry 18)

Column chromatography on silica gel (EtOAc–n-hexane, 2:1) afforded the product as a white solid; yield: 1.64 g (64%); mp 218.5 °C.

IR (KBr): 3036, 2972, 1720, 1707, 1648, 1451 cm⁻¹.

¹H NMR (250 MHz, CDCl₃): δ = 3.61 (s, 3 H, N3-CH₃), 3.94 (s, 3 H, N7-CH₃), 7.22–7.26 (m, 2 H_{arom}), 7.44–7.50 (m, 3 H_{arom}), 7.55 (s, 1 H, H-8, theobromine).

¹³C NMR (62.5 MHz, CDCl₃): δ = 27.12, 31.25, 106.53, 123.29, 125.83, 129.16, 130.35, 146.50, 148.07, 150.64, 165.70.

MS (EI): m/z = 256 (19.8, [M⁺]).

Anal. Calcd for C₁₃H₁₂N₄O₂: C, 60.93; H, 4.72; N, 21.86. Found: C, 60.98; H, 4.81; N, 21.80.

1-(4-Methoxyphenyl)-3,7-dimethyl-1H-purine-2,6(3H,7H)-dione (Table 4, entry 19)

Column chromatography on silica gel (EtOAc–n-hexane, 2:1) afforded the product as a white solid; yield: 1.94 g (68%); mp 182.5 °C.

IR (KBr): 3050, 2951, 1720, 1705, 1653, 1475, 1210 cm⁻¹.

¹H NMR (250 MHz, CDCl₃): δ = 3.59 (s, 3 H, N3-CH₃), 3.82 (s, 3 H, N7-CH₃), 3.95 (s, 3 H, OCH₃), 6.98 (d, J = 7.9 Hz, 2 H_{arom}), 7.13 (d, J = 7.9 Hz, 2 H_{arom}), 7.53 (s, 1 H, H-8, theobromine).

¹³C NMR (62.5 MHz, CDCl₃): δ = 28.36, 30.16, 53.91, 105.48, 115.03, 122.81, 124.20, 144.85, 149.26, 151.27, 157.31, 164.62.

MS (EI): m/z = 286 (16.2, [M⁺]).

Anal. Calcd for C₁₄H₁₄N₄O₃: C, 58.73; H, 4.93; N, 19.57. Found: C, 58.65; H, 4.98; N, 19.43.

Acknowledgment

We thank Shiraz University of Technology and Shiraz University Research Councils for partial support of this work.

References

- (1) Sherington, D. C. In *Supported Reagents and Catalyst in Chemistry*; Hodnett, B. K.; Kybett, A. P.; Clark, J. H.; Smith, K., Eds.; Royal Society of Chemistry: Cambridge, **1998**, 220–228.
- (2) Soai, K.; Watanabe, M.; Yamamoto, A. *J. Org. Chem.* **1990**, 55, 4832.

- (3) Joseph, T.; Deshpande, S. S.; Halligudi, S. B.; Vinu, A.; Ernst, S.; Hartmann, M. *J. Mol. Catal. A: Chem.* **2003**, *206*, 13.
- (4) Joseph, T.; Halligudi, S. B. *J. Mol. Catal. A: Chem.* **2005**, *229*, 241.
- (5) Meldal, M.; Tornøe, C. W. *Chem. Rev.* **2008**, *108*, 2952.
- (6) Beletskaya, I. P.; Cheprakov, A. V. *Coord. Chem. Rev.* **2004**, *248*, 2337.
- (7) Girard, C.; Onen, E.; Aufort, M.; Beauvière, S.; Samson, E.; Erscofici, J. *Org. Lett.* **2006**, *8*, 1689.
- (8) (a) Lipshutz, B.; Taft, B. R. *Angew. Chem. Int. Ed.* **2006**, *45*, 8235. (b) Sharghi, H.; Khalifeh, R.; Doroodmand, M. M. *Adv. Synth. Catal.* **2009**, *351*, 207.
- (9) Reddy, K. R.; Kumar, N. S.; Sreedhar, B.; Kantam, M. L. *J. Mol. Catal. A: Chem.* **2006**, *252*, 136.
- (10) (a) Chassing, S.; Kumarraja, M.; Sido, A. S. S.; Pale, P.; Sommer, J. *Org. Lett.* **2007**, *9*, 883. (b) Maurya, M. R.; Chandrakar, A. K.; Chand, S. *J. Mol. Catal. A: Chem.* **2007**, *274*, 192.
- (11) Kantam, M. L.; Jaya, V. S.; Sreedhar, B.; Rao, M. M.; Choudary, B. M. *J. Mol. Catal. A: Chem.* **2006**, *256*, 273.
- (12) (a) Li, P.; Wang, L.; Zhang, Y. *Tetrahedron* **2008**, *64*, 10825. (b) Likhari, P. R.; Roy, S.; Roy, M.; Kantam, M. L.; De R, L. *J. Mol. Catal. A: Chem.* **2007**, *271*, 57.
- (13) (a) Corma, A.; Garcia, H. *Chem. Rev.* **2002**, *102*, 3837. (b) Wight, A. P.; Davis, M. *Chem. Rev.* **2002**, *102*, 3589. (c) De Vos, D. E.; Dams, M.; Sels, B. F.; Jacobs, P. A. *Chem. Rev.* **2002**, *102*, 3615.
- (14) (a) Garg, B. S.; Sharma, R. K.; Bhojak, N.; Mittal, S. *J. Microchem.* **1999**, *61*, 94. (b) Sharma, R. K.; Mittal, S.; Koel, M. *Crit. Rev. Anal. Chem.* **2003**, *33*, 183.
- (15) (a) Bedford, R. B.; Singh, U. G.; Walton, R. I.; Williams, R. T.; Davis, S. A. *Chem. Mater.* **2005**, *17*, 701. (b) Paul, S.; Clark, J. H. *J. Mol. Catal. A: Chem.* **2004**, *215*, 107. (c) Horniakova, J.; Raja, T.; Kubota, Y.; Sugi, Y. *J. Mol. Catal. A: Chem.* **2004**, *217*, 73. (d) Jones, C. W.; McKittrick, M. W.; Nguyen, J. V.; Yu, K. *Top. Catal.* **2005**, *34*, 67. (e) Karimi, B.; Ma'Mani, L. *Org. Lett.* **2004**, *6*, 4813. (f) Cao, W.; Zhang, H. B.; Yuan, Y. *Z. Catal. Lett.* **2003**, *91*, 243. (g) Horniakova, J.; Nakamura, H.; Kawase, R.; Komura, K.; Kubota, Y.; Sugi, Y. *J. Mol. Catal. A: Chem.* **2005**, *233*, 49. (h) Al-Hashimi, M.; Fisset, E.; Sullivan, A. C.; Wilson, J. R. H. *Tetrahedron Lett.* **2006**, *47*, 8017.
- (16) (a) Craig, P. N. In *Comprehensive Medicinal Chemistry*, Vol. 8; Drayton, C. J., Ed.; Pergamon: New York, **1991**. (b) Southon, I. W.; Buckingham, J. In *Dictionary of Alkaloids*; Saxton, J. E., Ed.; Chapman & Hall: London, **1989**. (c) Negwer, M. *Organic-Chemical Drugs and their Synonyms*, 8th ed.; Wiley-VCH: Weinheim, **2002**.
- (17) (a) Legraverend, M.; Grierson, D. S. *Bioorg. Med. Chem.* **2006**, *14*, 3987. (b) Strouse, J. J.; Jelnik, M.; Arterburn, J. B. *Acta Chim. Slov.* **2005**, *52*, 187. (c) Williams, M.; Jarvis, M. F. *Biochem. Pharmacol.* **2000**, *59*, 1173. (d) Davis, J. T. *Angew. Chem. Int. Ed.* **2004**, *43*, 668.
- (18) (a) Hocek, M. *Eur. J. Org. Chem.* **2003**, *2*, 245. (b) Lister, J. H. In *The Chemistry of Heterocyclic Compounds*, Vol. 24; Weissberger, A.; Taylor, E. C., Eds.; Wiley-Interscience: New York, **1971**. (c) Shaw, G. In *Comprehensive Heterocyclic Chemistry*, Vol. 5; Katritzky, A. R.; Rees, C. W., Eds.; Pergamon: New York, **1984**. (d) Gabel, N. W.; Binkley, S. B. *J. Org. Chem.* **1958**, *23*, 643. (e) Greenberg, S. M.; Ross, L. O.; Robins, R. K. *J. Org. Chem.* **1959**, *24*, 1314. (f) El-Bayouki, K. A. M.; El-Sayed, A. S.; Basyouni, W. M. *Gazz. Chim. Ital.* **1989**, *119*, 163. (g) Taylor, E. C.; Yoneda, F. *J. Org. Chem.* **1972**, *37*, 4464.
- (19) (a) Stig, A. J.; Synne, R.; Tore, B. *J. Chem. Soc., Perkin Trans. 1* **1999**, 3265. (b) Zhou, T.; Li, T.-C.; Chen, Z.-C. *Helv. Chim. Acta* **2005**, *88*, 290.
- (20) (a) Gondela, A.; Walczak, K. *Tetrahedron: Asymmetry* **2005**, *16*, 2107. (b) Boga, C.; Bonmartini, A. C.; Forlani, L.; Modarelli, V.; Righi, L.; Sgarabotto, P. *J. Chem. Res., Miniprint* **2001**, 1217. (c) Khalafi-Nezhad, A.; Zare, A.; Parhami, A.; Soltani Rad, M. N.; Nejabat, G. R. *Can. J. Chem.* **2006**, *84*, 979. (d) Khalafi-Nezhad, A.; Zare, A.; Parhami, A.; Soltani Rad, M. N.; Nejabat, G. R. *Synth. Commun.* **2006**, *36*, 3549. (e) Zare, A.; Hasaninejad, A.; Moosavi-Zare, A. R.; Beyzavi, M. H.; Khalafi-Nezhad, A.; Pishahang, N.; Parsaee, Z.; Mahdaviniasab, P.; Hayati, N. *ARKIVOC* **2008**, (xvi), 178.
- (21) (a) Ding, S.; Gray, N. S.; Ding, Q.; Schultz, P. G. *Tetrahedron Lett.* **2001**, *42*, 8751. (b) Bakkestuen, A. K.; Gundrersen, L.-L. *Tetrahedron Lett.* **2003**, *44*, 3359. (c) Yue, Y.; Zheng, Z.-G.; Wu, B.; Xia, C.-Q.; Yu, X.-Q. *Eur. J. Org. Chem.* **2005**, *24*, 5154. (d) Bakkestuen, A. K.; Gundrersen, L.-L.; Utenova, B. T. *J. Med. Chem.* **2005**, *48*, 2710. (e) Jacobsen, M. F.; Knudsen, M. M.; Gothelf, K. V. *J. Org. Chem.* **2006**, *71*, 9183. (f) Tao, L.; Yue, Y.; Zhang, J.; Chen, S.-Y.; Yu, X.-Q. *Helv. Chim. Acta* **2008**, *91*, 1008. (g) Keder, R.; Dvořáková, H.; Dvořák, D. *Eur. J. Org. Chem.* **2009**, *10*, 1522. (h) Huang, H.; Liu, H.; Chen, K.; Jiang, H. *J. Comb. Chem.* **2007**, *9*, 197. (i) Kim, D.; Lee, H.; Jun, H.; Hong, S.-S.; Hong, S. *Bioorg. Med. Chem.* **2011**, *19*, 2508.
- (22) (a) Soltani Rad, M. N.; Khalafi-Nezhad, A.; Behrouz, S.; Faghihi, M. A.; Zare, A.; Parhami, A. *Tetrahedron* **2008**, *64*, 1778. (b) Soltani Rad, M. N.; Khalafi-Nezhad, A.; Behrouz, S.; Asrari, Z.; Behrouz, M.; Amini, Z. *Synthesis* **2009**, 3067. (c) Soltani Rad, M. N.; Khalafi-Nezhad, A.; Behrouz, S. *Helv. Chim. Acta* **2009**, *92*, 1760. (d) Soltani Rad, M. N.; Khalafi-Nezhad, A.; Behrouz, S. *Beilstein J. Org. Chem.* **2010**, *6*, No. 49. (e) Khalafi-Nezhad, A.; Soltani Rad, M. N.; Moosavi-Movahedi, A. A.; Kosari, M. *Helv. Chim. Acta* **2007**, *90*, 730. (f) Khalafi-Nezhad, A.; Soltani Rad, M. N.; Khoshnood, A. *Synthesis* **2004**, 583. (g) Khalafi-Nezhad, A.; Soltani Rad, M. N.; Hakimelahi, G. H.; Mokhtari, B. *Tetrahedron* **2002**, *58*, 10341. (h) Khalafi-Nezhad, A.; Zare, A.; Soltani Rad, M. N.; Mokhtari, B.; Parhami, A. *Synthesis* **2005**, 419. (i) Khalafi-Nezhad, A.; Zare, A.; Parhami, A.; Soltani Rad, M. N. *ARKIVOC* **2006**, (xii), 161.
- (23) (a) Zolfigol, M. A. *Tetrahedron* **2001**, *57*, 9509. (b) Shaterian, H. R.; Ghashang, M.; Feyzi, M. *Appl. Catal., A* **2008**, *345*, 128.
- (24) Xue, B.; Chen, P.; Hong, Q.; Lin, J.; Tan, K. L. *J. Mater. Chem.* **2001**, *11*, 2378.
- (25) Topnani, N.; Kushwaha, S.; Athar, T. *Int. J. Green Nanotechnol., Mater. Sci. Eng.* **2009**, *1*, M67.
- (26) (a) Kim, D.; Jun, H.; Lee, H.; Hong, S.-S.; Hong, S. *Org. Lett.* **2010**, *12*, 1212. (b) Maheswaran, H.; Krishna, G. G.; Prasanth, K. L.; Srinivas, V.; Chaitanya, G. K.; Bhanuprakash, K. *Tetrahedron* **2008**, *64*, 2471.